JOURNAL OF MATERIALS SCIENCE **35** (2000) 1239–1252

Mechanism of primary nucleation and origin of hysteresis in the rotator phase transition of an odd *n*-alkane

K. NOZAKI*
Department of Physics, Faculty of Science, Yamaguchi University, 1677-1 Yoshida, Yamaguchi 753-8512, Japan
E-mail: nozaki@sci.yamaguchi-u.ac.jp

M. HIKOSAKA
Division of Material and Life Sciences, Faculty of Integrated Arts and Sciences, Hiroshima University, Higashi-Hiroshima, Hiroshima 739-8521, Japan
E-mail: hikosaka@ue.ipc.hiroshima-u.ac.jp

The rotator phase transition in *n*-alkane single crystal was investigated mainly by means of *in situ* optical microscopy. It was found that 'wrinkles' appeared on heating at a temperature slightly below the transition point, and that the rotator phase grew from the wrinkle. It is proposed that the appearance of the winkle is a precursor of the transition. The nucleus of the rotator phase was considered to be formed in the wrinkle. The nucleation rate of the primary nucleus of the rotator phase was also measured. The primary nucleation rate was found to be proportional to $\exp(-C/\Delta T^2)$, which means that the primary nucleus is three-dimensional one. It was concluded from the results of the morphological observation and the consideration of the observed C value that the primary nucleus is heterogeneously formed in the precursor winkle and that the rotator phase transition is controlled by the nucleation and growth. On cooling, on the other hand, no precursor was observed prior to the transition, and significant large supercooling was observed. This type of hysteresis is commonly observed in the first-order phase transitions in materials. It was shown that the origin of the hysteresis has close relation to the mechanism of the primary nucleation. A universal model of the origin of the hysteresis was proposed, and the tangible evidence of it was shown in the case of *n*-alkane.

1. Introduction

First-order phase transitions, such as melting and crystallization, solid-solid phase transition, etc., are important phenomena not only for material sciences but for material engineering. Therefore, there have been many studies on the first-order phase transitions, however, several unsolved problems remain. Those are, for example, the kinetics of the solid-solid phase transition and the hysteresis which is characterized by the difference in observed transition temperatures between on heating and on cooling. With regards to the kinetics of the solid-solid phase transition, there have been a little studies, which are mainly theoretical ones, because it was difficult to observe the changes during the solid-solid transition which usually completes in a short time. With regards to the hysteresis, the origin of it have not been revealed using experimental evidence yet. In our previous work [1], the kinetics of the growth during the solid-solid phase transition of *n*-alkane was investigated and it was shown for the first time that the growth was mainly controlled by the two-dimensional (2D) nucleation during the solid-solid phase transition.

In this work, it will be proposed that the primary nucleation in the phase transition of *n*-alkane on heating is accelerated by a kind of precursor, which is observed below the transition temperature as an appearance of 'wrinkles,' although there will be remained a little another possibility that the 'wrinkle' is not a precursor but the onset of the transition cased by an impurity effect which lowers the transition point. It will be also shown that the hysteresis is due to a difference in mechanism of primary nucleation between on heating and on cooling. The purposes of this work are to reveal the mechanism of the primary nucleation in the solid-solid phase transition of *n*-alkane and to show a tangible experimental evidence of the hysteresis.

1.1. Phase transitions of long chain compounds and polymers

The rate of the solid-solid phase transition in long chain compounds and polymer materials is considered to be

* Author to whom all correspondence should be addressed.

smaller than that in low molecular weight materials. Therefore it may be possible to observe changes during the transition in long chain compounds and polymers. Furthermore, the hysteresis seems to be more remarkable with increase in molecular weight. For example in crystalline polymers, the observed crystallization temperature is about a few tens degrees lower than the observed melting temperature [2]. Furthermore, in the crystal of a normal higher alcohol, the marked hysteresis is observed in the order-disorder type transition [3]. Takamizawa, *et al.* [4] reported that the freezing phenomenon of a high-temperature phase was observed in longer *n*-alkane when the sample was cooled to room temperature. This is an extreme case, in which the transition temperature is depressed below room temperature.

Normal alkane is the simplest of the linear hydrocarbon molecules, and is often regarded as the model molecule of other hydrocarbons. Therefore, we will investigate here *n*-alkane, *n*-pentacosane (n-$C_{25}H_{52}$: C25).

1.2. Normal alkane

Linear hydrocarbon molecules, such as lipids, oils and polymers, often show characteristic crystalline phases, which are commonly called rotator phases (R phases), just below their melting points [5]. A crystal of *n*-alkane also shows the first order phase transition which we call the rotator phase transition (the R phase transition) between the low-temperature ordered (LO) phase and the R phase [6, 7].

In the LO phase, *n*-alkane molecules are fully extended taking *all-trans* conformations and are registrated in layers in which the molecular chain axes are parallel with each other, having the long range order with respect to the orientation about their long axes. In the R phase, the *all-trans* conformation of the molecules is partially deformed. The crystal still have three-dimensional long range positional order crystallographically, but lack the long range order in the orientation about their long axes. Recent X-ray investigations have shown the presence of five R phases which have different structures [8–15].

The molecules of *n*-alkane in the R phase behave as if they were in a liquid crystalline state and have high mobility. The long range diffusion of the molecules are observed by means of X-ray powder diffraction [16] and optical microscopy [17, 18]. These characteristics are considered to be related to various function of biological membranes. Hence, in recent years, there has been a growing interest in the R phase.

It is well-known that crystal structure and phase behavior of material are usually influenced by an impurity. In the case of *n*-alkane system, the important impurities are homologous molecules. The binary system of *n*-alkane, when the difference in the number of carbon atoms of the two components is small (within about four), shows the formation of the solid-solution in the LO phase, in which the crystal structure is different from than that of pure alkane [19, 20]. The LO-R phase transition temperature is also lowered in the alkane binary system. Hence, the pure *n*-alkane sample is contaminated with small amount (less than wt%) of homologous impurity, the impurity molecules are well-mixed with pure alkane molecules even in the LO phase resulting in lowering of the transition point. In fact, this effect is more significant for the transitions among the LO phases [21] than for the LO-R transition.

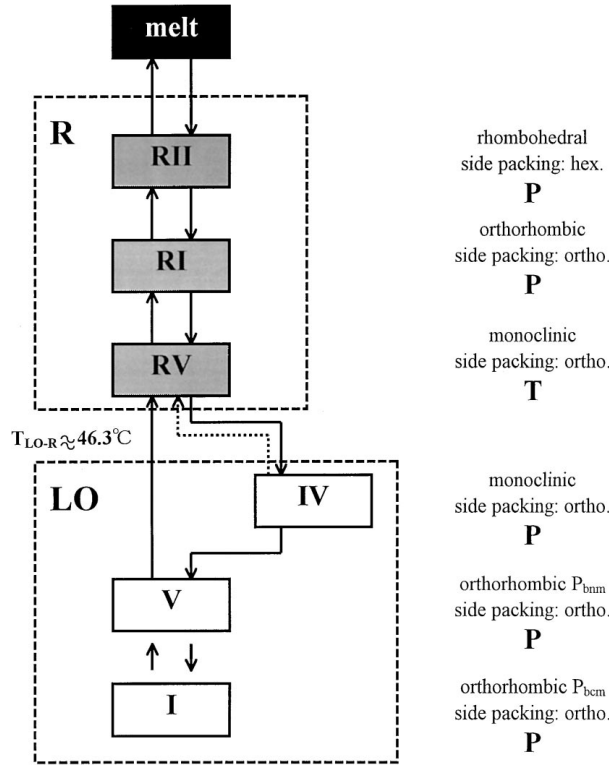

Figure 1 Schematic picture of the phase behavior of C25. The T and P mean that the molecules are perpendicular to the layer surface and tilt from the normal to the layer surface, respectively. Phases I, V, and IV are the LO phases and the RV, RI, and RII are R phases.

1.3. Phase transitions and crystal structures in C25

The phase behavior of *n*-alkane depends on its carbon number. Fig. 1 shows the phase transitions in C25. The transitions I→V→RV→RI→RII and RII→RI→RV→IV→V→I are observed during heating and cooling, respectively [14, 22, 23], where I, V, and IV are the LO phases, and RV, RI, and RII are the R phases.

It is to be noted that phase IV appears only on cooling. In *n*-alkane crystals the phase transitions within the LO phases sensitively depend on the purity of the sample [21]. In our previous experiment using C25 with poor purity, phase IV was observed even on heating by means of X-ray diffraction [22]. However, when sample with high purity (99.9 wt%) is used, phase IV does not appear on heating in C25 [23].

In all LO phases of C25, the side packing is orthorhombic (herringbone type), which is the same as that in the orthorhombic crystal of polyethylene, and the molecular chain axes are perpendicular to the layer surface, but only the layer stackings are different [22, 24]. The RV and RI phase have the same orthorhombic side packing, but the molecules in the RV phase are tilt

from the layer surface normal [14]. In the RII phase, the side packing is hexagonal, and the chain axes are perpendicular to the layer surface.

1.4. Thermal expansion of the lattice in *n*-alkane crystal

Orthorhombic *n*-alkane with herringbone side packing usually shows larger thermal expansion of the lattice along the *a* axis compared with that in other directions, where *a*, *b* and *c* are defined to the subcell, in which the *c* axis is parallel to the the chain axis, and the *a* and *b* axes are perpendicular to the chain axis. The lattice constant *a* shows a significant increase among the LO phase with increasing temperature, and jump at the R phase transition [9, 12]. The lattice constant *b* also increases with increasing temperature among the LO phase, but the expansion coefficient is smaller than that of *a*. At the R phase transition, the *b* decreases discontinuously. It will be discussed in this paper that the difference in expansion of the lattice have relevance with the origin of the precursor wrinkles.

1.5. Purpose

In this study, we focus on the R phase transition ($\mathrm{LO}\underset{\rightarrow}{\leftarrow}\mathrm{R}$) in C25 crystal. The change in the morphology was observed during the transition using *in situ* optical microscope. The results will show that the wrinkles appear parallel to the *b* axis prior to the R phase transition and the primary nucleus of the R phase is considered to be formed in the wrinkles, because it was observed by means of the optical microscopy that the R phases always grew from the wrinkles. The nucleation rate of the primary nucleus of the R phase was also measured. It will be concluded from the morphological change during the transition and the temperature dependence of the nucleation rate that the primary nucleation is three-dimensional and heterogeneous one.

The typical hysteresis is observed in the R phase transition. The observed transition temperature in cooling $T_{\mathrm{R-LO}}$ is a few degrees lower than that on heating $T_{\mathrm{LO-R}}$. In the present case, $T_{\mathrm{LO-R}}$ is considered to be approximately equal to the equilibrium transition temperature $T^0_{\mathrm{LO-R}}$, (the reason of this will be discussed in this paper). In other words, superheating is not significant, but a few degrees of supercooling is observed. The origin of the hysteresis will be discussed relating to the mechanism of the primary nucleation.

2. Experimental

Normal pentacosane (C25) were purchased from Tokyo Kasei Kogyo Co., Ltd. The purity was about 99.6 wt% according to capillary gas chromatography. The sample used here was purer than that used in our previous study [22]. Most of the impurities were homologous molecules, which were *n*-$C_{24}H_{50}$ (0.07 wt%), *n*-$C_{26}H_{54}$ (0.04 wt%), *n*-$C_{27}H_{56}$ (0.07 wt%) and unsaturated (or branched) $C_{25}H_x$ (0.22 wt%). Single-crystal plates (30–150 μm thick) were prepared from *p*-xylene solution by slow evaporation of the solvent at room temperature, where C25 crystallizes into phase I. The surface of the sample plate corresponds to the *ab* plane of the orthorhombic unit cell; the molecular chain axes are perpendicular to the plate surface.

Differential scanning calorimetry (DSC) and X-ray powder diffraction are made in order to investigate the phase behavior of the C25 sample used in this experiment. DSC was performed with a standard apparatus (Rigaku, DSC8230) using single crystals as initial samples with various heating and cooling rate.

The powder sample for X-ray diffraction experiment was prepared by crashing the single crystals. X-ray powder diffraction was made by Debye-Scherrer method using X-ray diffraction system with imaging plates (Mac Science, DIP220). The Cu-K_α radiation (40 kV, 250 mA) was used. The time for exposure was five minutes at each temperature every 0.2°C, the effective heating and cooling rate was about 0.04 °C/min. The temperature of the sample was controlled within ±0.1°C.

The specimen for optical observation was placed on a hot stage (LINKAM, LK600PH), the temperature of which was controlled by a PID controller; the fluctuation of the temperature was less than 0.025°C. *In situ* optical observation was made using a polarizing microscope with crossed nicols. The optical images was stored in a video tape through a CCD camera (Tokyo Electric Industry Co., Ltd.) for five minutes at each temperature every 0.1°C around the transition, the effective heating and cooling rate was about 0.02 °C/min. In another case, isothermal measurements for several hours were made.

The nucleation rate was measured by using optical microscope. The single crystal sample was quickly heated from a temperature below $T_{\mathrm{LO-R}}$ to that above $T_{\mathrm{LO-R}}$ during the measurement.

The transition temperature $T_{\mathrm{LO-R}}$ was determined from the results of DSC measurements with various heating rate. The $T_{\mathrm{LO-R}}$ is also confirmed by means of X-ray diffraction and optical microscopy in this study. The R phase transition results in high optical isotropization around the chain axis, giving rise to dark regions under crossed nicols. While during the transitions between the LO phases, no change in optical image is detected.

The morphology of the crystal surface, which was coated with gold, was observed at room temperature using a scanning electron microscope (SEM) (JEOL: JSM-T200) with a beam of electrons accelerated by the voltage of 15 kV.

3. Results

3.1. DSC

Fig. 2a shows the DSC heating and cooling thermograms of C25. The observed peaks correspond to the phase transitions I→V→RV→RI→RII→melt on heating and melt →RII→RI→RV→IV→V→I on cooling, respectively. Phase IV was confirmed only on cooling. Fig. 2b shows the observed transition temperature on heating determined from the results of DSC measurements. The transition temperature does

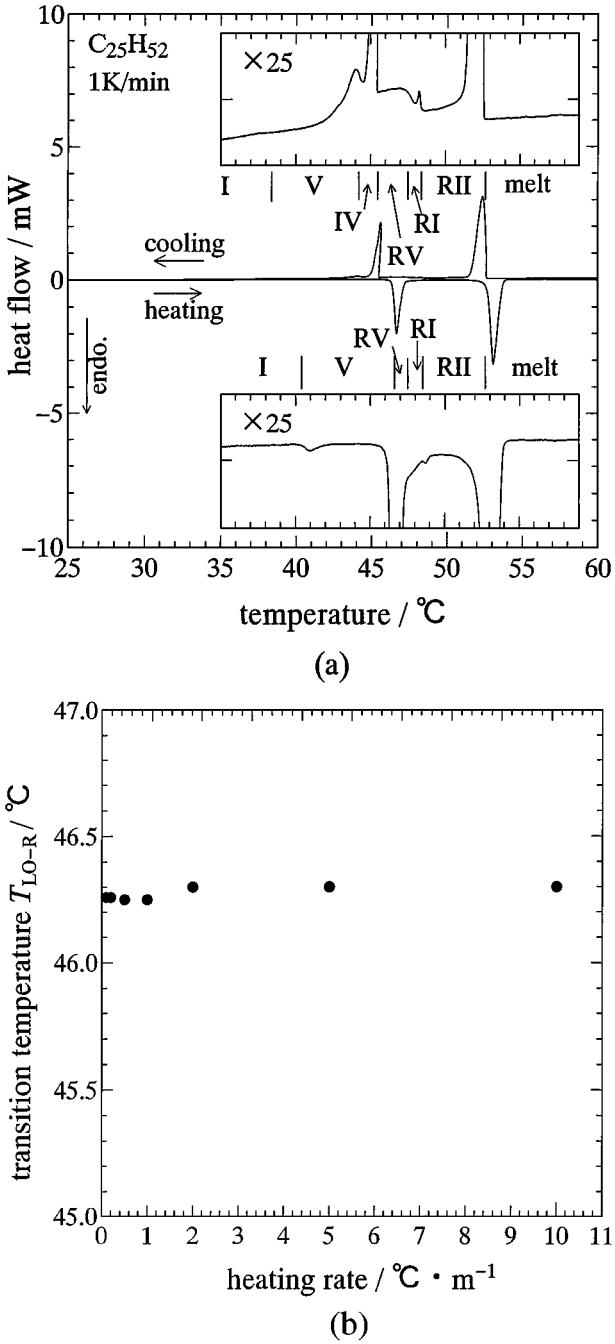

Figure 2 (a) DSC thermograms of C25 on heating and on cooling. The observed peaks correspond to the I→V→RV→RI→RII→melt transition on heating and the melt →RII→RI→RV→IV→V→I on cooling. (b) The observed transition temperature various heating and cooling rate determined by DSC measurement.

not show significant dependence on the heating rate. This means that the observed transition temperature T_{LO-R} is approximately equal to the equilibrium transition temperature T^0_{LO-R}, i.e. $T_{LO-R} = T^0_{LO-R}$. We determined the transition temperature as $T_{LO-R} = 46.3°C$. The supercooling of 1°C was observed in the R phase transition.

3.2. X-ray diffraction

The result of X-ray powder diffraction was consistent with that of DSC and is shown in Fig. 3a and b. The transition temperature $T_{LO-R} = 46.3°C$ was confirmed. The supercooling of 1–1.3°C was observed on cooling. It clearly showed that phase IV appeared only on cooling as well as during the DSC measurement in the C25 sample used here. This is due to high purity of the present sample.

Fig. 3c shows the change in lattice constants *a* and *b* of C25 on heating determined by means of X-ray diffraction. This result is consistent with the previous works by Doucet, *et al.* [8] and Ungar [13]. The lattice constant *a* shows an increase of about 1% with increasing in temperature in the LO phase, while the lattice constant *b* shows an smaller increase of about 0.2%.

3.3. Optical observation on heating

Fig. 4 shows a series of schematic illustrations of the observed change in morphology during the transition. A series of corresponding optical photographs are also shown in Fig. 5a–i, where (a), (b), ··· correspond to those in Fig. 4. When the crystal in the LO phase (Fig. 5a) was heated to a temperature 0.5–1.0°C below 46.3°C ($=T_{LO-R}$), many wrinkles appeared parallel to the *b* axis (Fig. 5b at 45.8°C). No change was observed in the optical image after holding the temperature at 45.8°C for a day. In a previous paper [25], we took these wrinkles for 'cracks' and suggested that the transition had already begun at this temperature. However, these were identified as wrinkles from the SEM.

The observed results of the appearance of the wrinkles may be interpreted several ways, 1. it is the occurrence of the transition among the LO phase, the V→IV transition, 2. it is the occurrence of the R phase transition, the V→IV transition, 3. it is a precursor of the R phase transition. In this work, we conclude the appearance of the wrinkles to be a precursor (3), and the details will be discussed in §Discussion.

Fig. 6 shows the temperature dependence of the density of the wrinkle. With increasing temperature up to T_{LO-R}, the number of wrinkle increased. Being cooled to room temperature, most of the wrinkles disappeared. When the crystal was heated again, the wrinkles always appeared at the same positions. At T_{LO-R}, the increase in wrinkle density was saturated. All the data of the wrinkle density of a few different samples (sample 1–sample 3) lie approximately on one well-defined curve, i.e. the density of the wrinkle is independent of the sample crystallized under the same condition. These phenomena may be closely related to the mechanism of the wrinkle formation.

Fig. 7a shows a SEM image of the wrinkles which happen to remain rarely at room temperature. SEM images of a typical wrinkle for various tilt angles (θ_{tilt}) of the sample were collected to investigate the three dimensional shape of the wrinkle. Geometry of this observation is illustrated in Fig. 7b. The typical images at $\theta_{tilt} = 20°$ and 60° are shown in Fig. 7c and d, respectively. The wrinkle morphology obtained from the SEM observation is schematically shown in Fig. 7e. The typical size of the wrinkle is about 3 μm wide, 0.5 μm high and several tens of micrometers long.

Fig. 5c shows the initial stage of the LO→R transition, where the dark R phase grows from the wrinkles. This temperature of 46.3°C corresponded to T_{LO-R} confirmed by means of DSC and X-ray diffraction. The

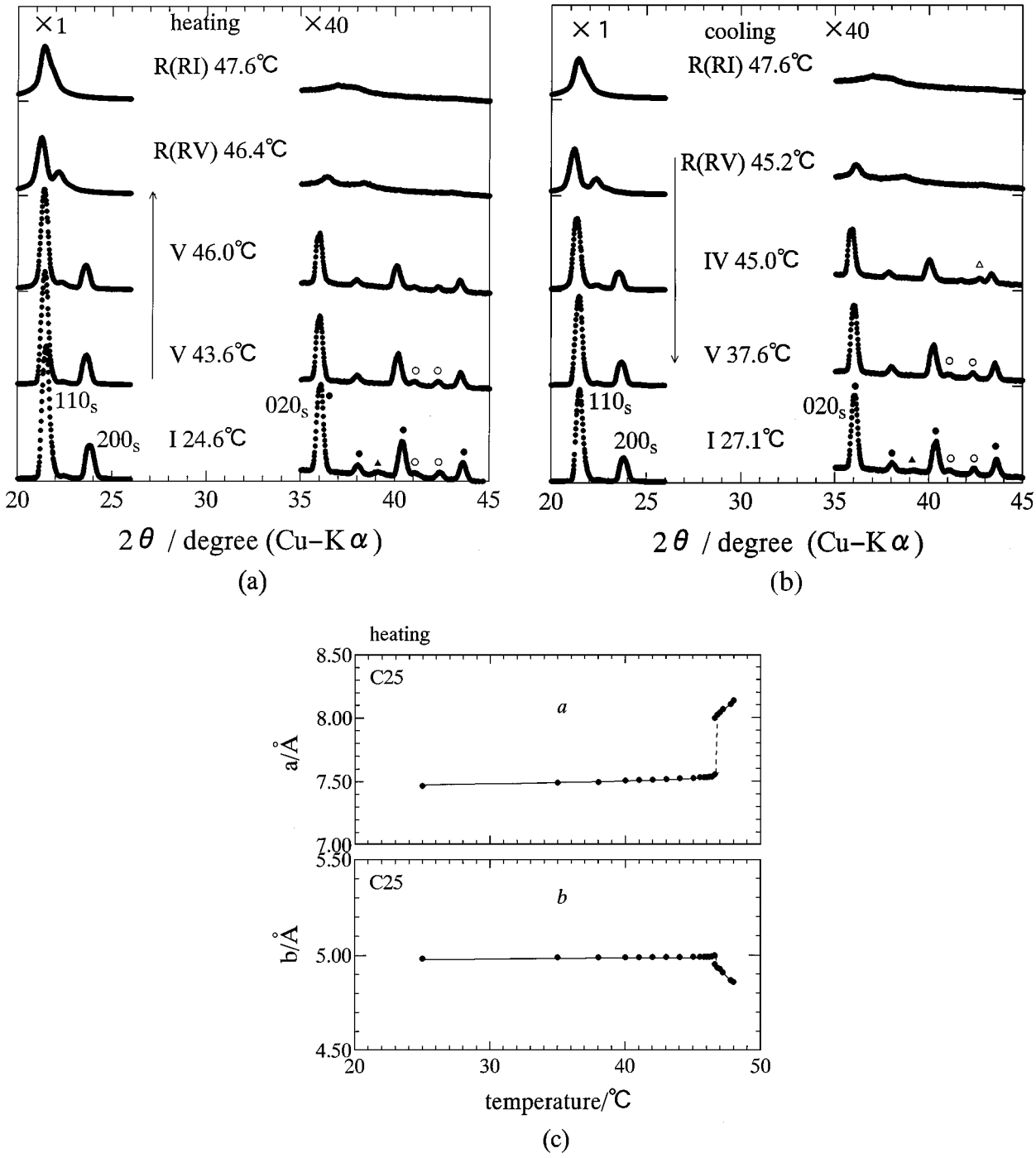

Figure 3 X-ray powder pattern of C25 at various temperature, (a) on heating and (b) on cooling. The 110_s, 200_s, 020_s are the reflections from the side packing. The full circle represents the reflections appearing in all LO phase, and the open circle represents reflections appearing both in phases I and V. The full triangle is the reflection appearing only in phase I, and the open triangle is the reflection appearing only in phase IV. The change in lattice constants *a* and *b* on heating (c). The lattice constants increase with increasing in temperature in the LO phase and show discontinuous change at the R phase transition. The change in *a* is larger than that in *b*.

growth of the R phase was observed only a temperature above 46.3°C. Therefore, this temperature was determined as the beginning temperature of the R phase transition (T_{LO-R}) by means of optical microscopy. The R phases always grew from the wrinkles, the R phase growing from other region was never observed. Thus we have conclusion from the *in situ* morphological observation that the primary nucleation process on heating during the R phase transition is heterogeneous one in the wrinkle. On the other hand, there were some wrinkles form which the R phase did not grow even at a high temperature (0.1–0.2 °C above 46.3°C). This fact indicates that the primary nucleus was not formed in such wrinkles yet, which is usual in the case of heterogeneous nucleation process.

As a time passes, the growth fronts, which are parallel to the *b* axis, translated along the *a* axis (Fig. 5d). This growth is controlled by 2D nucleation as has been concluded in a previous paper [1]. The growth front parallel to the *b* axis can be regarded as a kind of 'facet' which is characteristic morphology for 2D nucleation.

Finally, all regions of the crystal transformed into the R phase; the transition completed (Fig. 5e). After the completion of the R phase transition, new thick

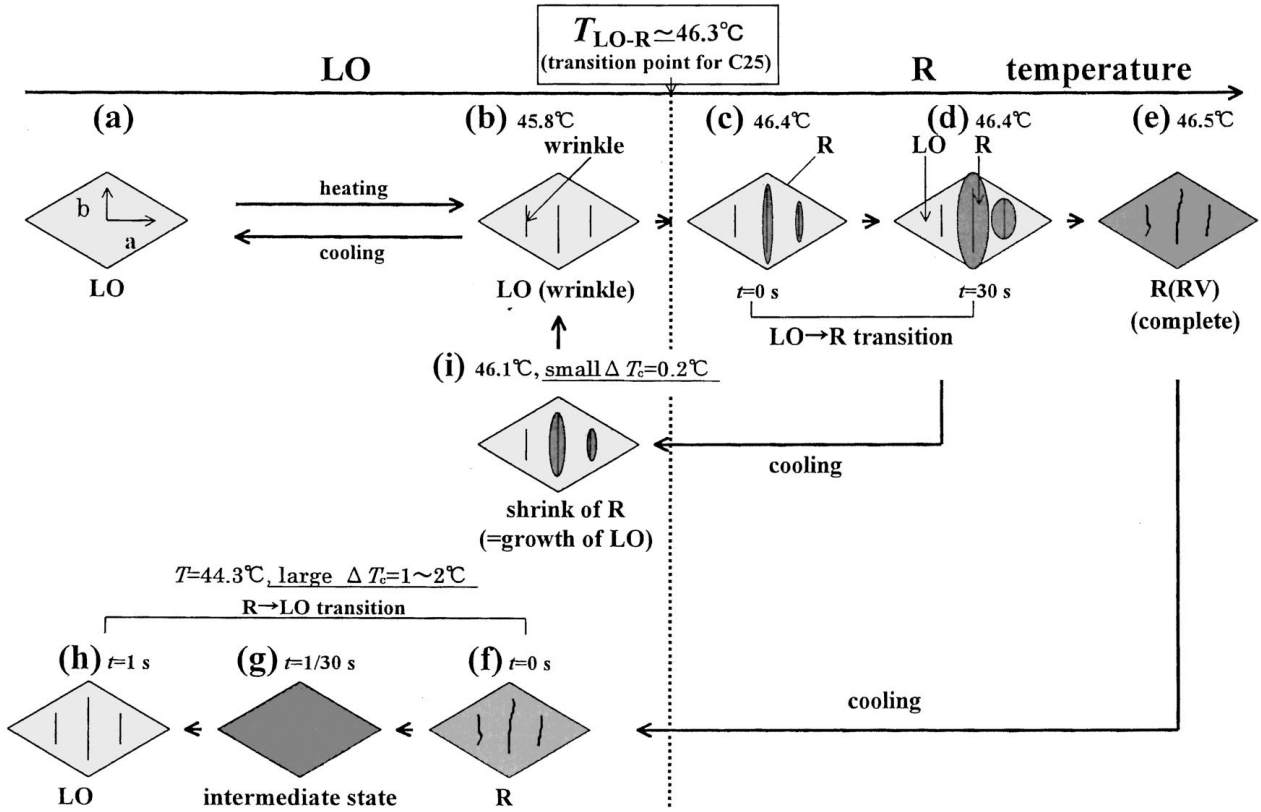

Figure 4 Schematic illustrations of the observed change in morphology of C25 during the LO-R transition. The lozenge indicates a single crystal of C25, in which the dark region and the vertical line represent the R phase and the wrinkle, respectively. The LO phase, which is phase V or IV in C25, appearing just below the R phase is depends on the sample purity.

wrinkles appeared on the R phase crystal. This type of wrinkle has already reported by Piesczek *et al.* [24], and is different from the 'precursor wrinkle' which appeared on the LO phase crystal below T_{LO-R}.

3.4. Primary nucleation rate

Fig. 8a shows the typical example of the density of the primary nucleus (ν) vs. time (t) at 46.45°C. When the growth of the dark R phase from the wrinkle was observed by means of optical microscopy, it was decided that the primary nucleus had been formed in the wrinkle. The nucleation rate (I) was estimated from the slope of the plots.

Fig. 8b shows log I vs. ΔT^{-2}, where ΔT is degree of superheating ($\Delta T \equiv T - T_{LO-R}$). This gives a straight line, hence we had an experimental formula,

$$I = I_0 \exp\left(-\frac{C}{\Delta T^{-2}}\right) \quad (1)$$

where C is a constant. It is well known that when the nucleation rate I is proportional to exp $(-C/\Delta T^2)$, this nucleation is mainly controlled by three dimensional (3D) nucleation process [26]. The C value estimated from the slope of the log I–ΔT^{-2} plot in Fig. 8b is

$$C_{obs} = 4.7 \times 10^{-2}\ \mathrm{K}^2. \quad (2)$$

This value is much smaller than the calculated C of the homogeneous nucleation $C_{homo} \simeq 7.1\mathrm{K}^2$, which will be shown in §Discussion. Therefore, this primary nucleation process is concluded to be heterogeneous one from the consideration of the nucleation rate.

3.5. Optical observation on cooling

When the sample in the R phase was cooled to a temperature slightly below T_{LO-R}, no change was observed. The crystal was in the supercooled R phase. Fig. 5f shows the R phase at 44.3°C in the supercooled state with $\Delta T_c = 2$°C, where ΔT_c is degree of supercooling ($\Delta T_c \equiv T_{LO-R} - T$). When the temperature was kept for 4–5 seconds at 44.3°C , the crystal suddenly transformed to the LO phase through a transient intermediate phase within 1 s (Fig. 5g, h) [25].

In another case of cooling, when the crystal was cooled from the state in which the LO→R transition had not completed, i.e. the LO and R phases coexisted, the R phase began shrinking (Fig. 5i). The LO phase began growing as soon as being cooled to a temperature below T_{LO-R}. The R→LO transition occurred with little supercooling, i.e. no significant supercooling was observed.

3.6. Hysteresis phenomenon

It is concluded from the results of the optical microscopy that the observed transition temperature is $T_{LO-R} = 46.3$°C on heating, while that on cooling from the R phase is $T_{R-LO} = 44.3$°C, which verified hysteresis. On heating, the wrinkles appeared on the crystal surface as a precursor of the transition, and the R phases nucleated and grew from the wrinkles. On cooling from

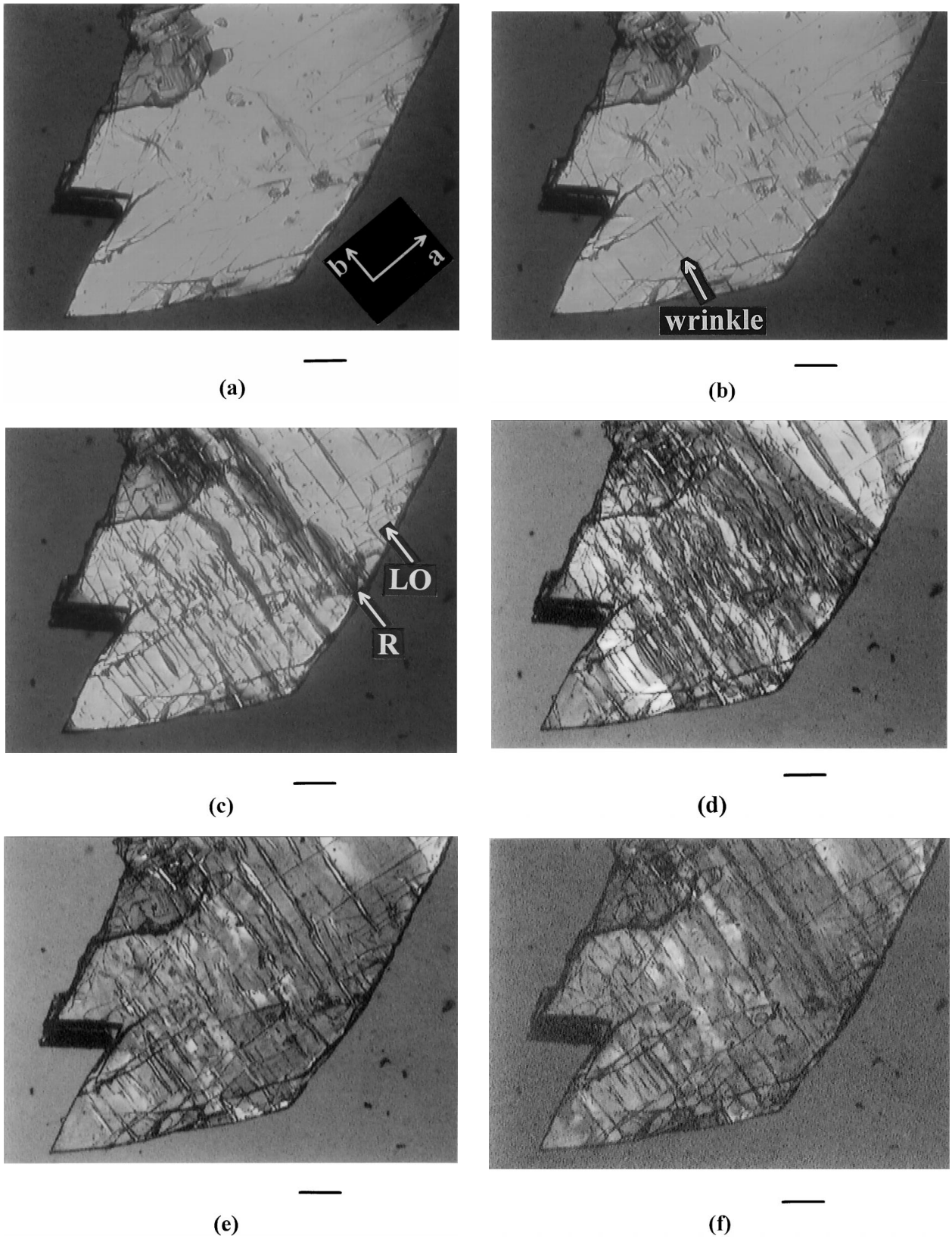

Figure 5 A series of optical photographs of the C25 single crystal undergoing the LO-R transition on heating: (a) at 44.0°C (LO), (b) at 45.8°C, (c) at 46.4°C, 0 s (LO→R), (d) at 46.4°C, 30 s and (e) at 46.5°C (R), and those on cooling at 44.3°C: (f) at 0 s (R), (g) at 1/30 s (intermediate state) and (h) at 1 s (LO). The photograph (i) shows the image at 46.1°C in the case of cooling from the state of (d). The photographs (a), (b), (c), . . . correspond to the pictures (a), (b), (c), . . . in Fig. 4, respectively. In all photographs, scale bar = 100 μm.(*Continued*).

the R phase, on the other hand, the transition suddenly began at a large ΔT_c without any precursor. In another case of cooling from the coexistent state of the LO and R phases, *i.e.* cooling from the state in which the LO→R transition had not completed, the R→LO transition occurred at a temperature below $T_{LO-R} = 46.3$°C without any degrees of supercooling. The significant hysteresis was not observed. This result also supports the

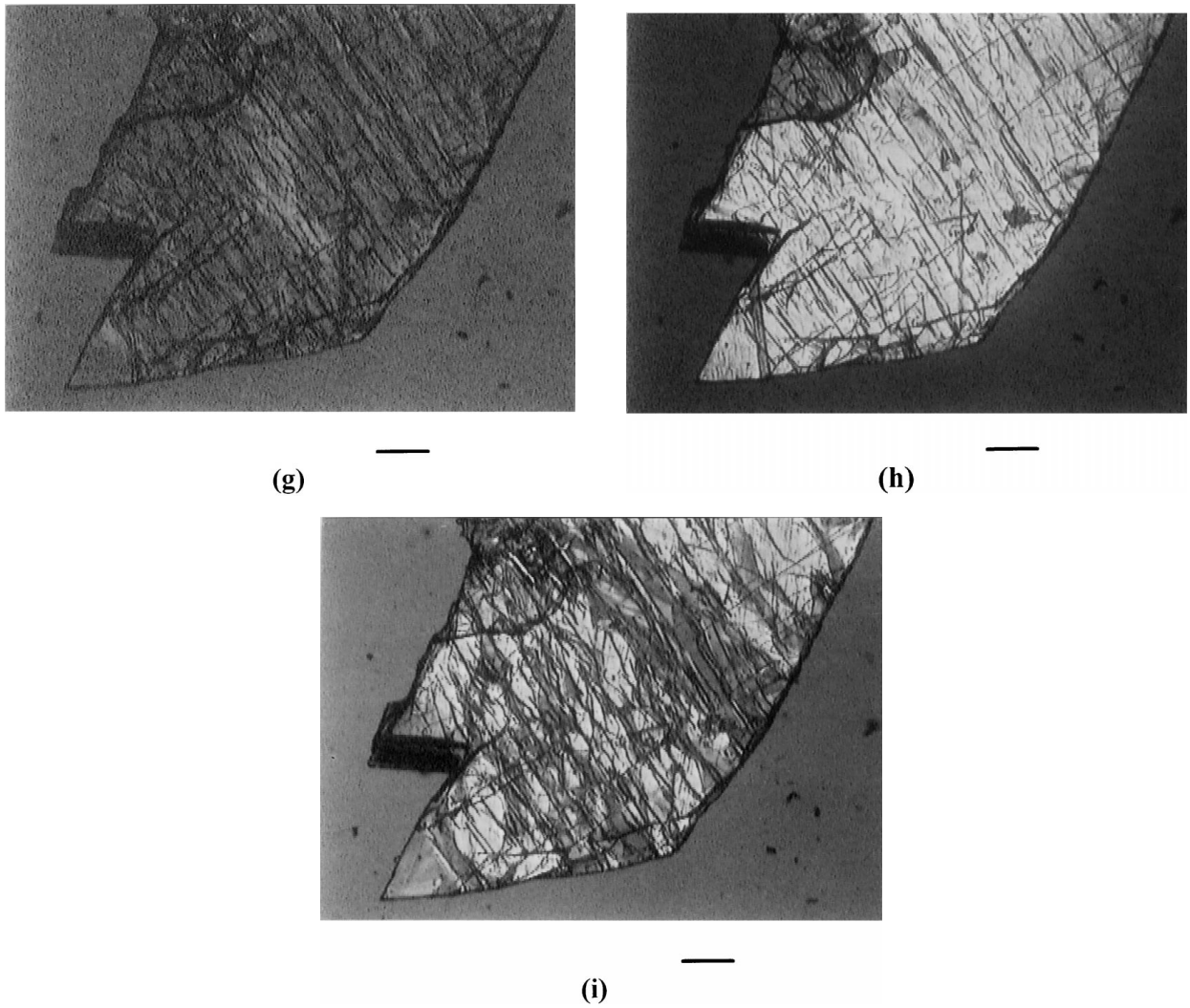

Figure 5 (*Continued*).

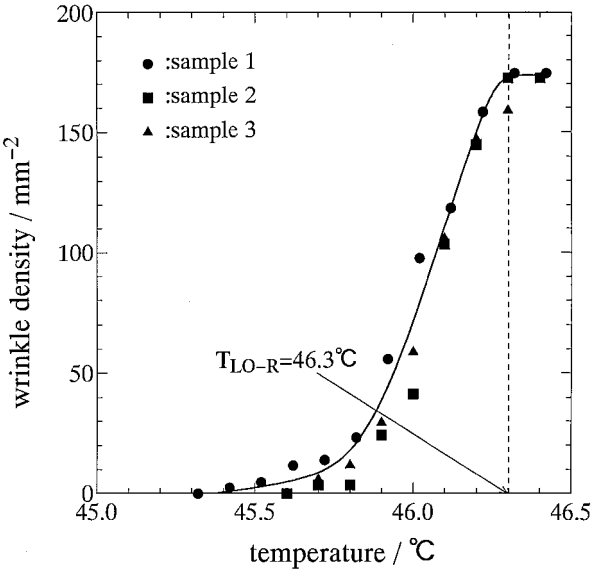

Figure 6 Temperature dependence of the density of the wrinkle. All data of the deferent samples (sample 1–sample 3) lie approximately on one curve.

assumption that $T_{LO-R} = T^0_{LO-R}$. In the latter case, the primary nucleation of the LO phase is not required. Thus, the origin of the hysteresis is expected to have relation to the mechanism of the primary nucleation.

4. Discussion

4.1. Precursor of the R phase transition?: wrinkle

Three possible explanations for the appearance of the wrinkle were supposed in §Results, 1. it is the onset of the V→IV transition, 2. it is the onset of the R phase transition, 3. it is a precursor of the R phase transition.

The crystal of C25 sometimes shows the V→IV transition below the R phase transition, when the sample has poor purity, as mentioned in §Introduction. However, the V→IV transition was not detected in this study on the sample with high purity. In addition, the wrinkles were also confirmed in the observation for *n*-$C_{23}H_{48}$ which never has phase IV [22]. Hence, the appearance of the wrinkle is not due to the V→IV transition.

If the appearance of the wrinkle was the onset of the R phase transition, the growth of the R phase should be observed in this case. However, in spite of holding the temperature for a day at 45.8°C, at which the wrinkles first appeared, the growth was never observed. The growth was confirmed only at a temperature above 46.3°C. Furthermore, since the R→LO transition began at a temperature just below 46.3°C in the case of cooling from the coexistent state of the LO phase and the R phase, hence the temperature of the 46.3°C considered

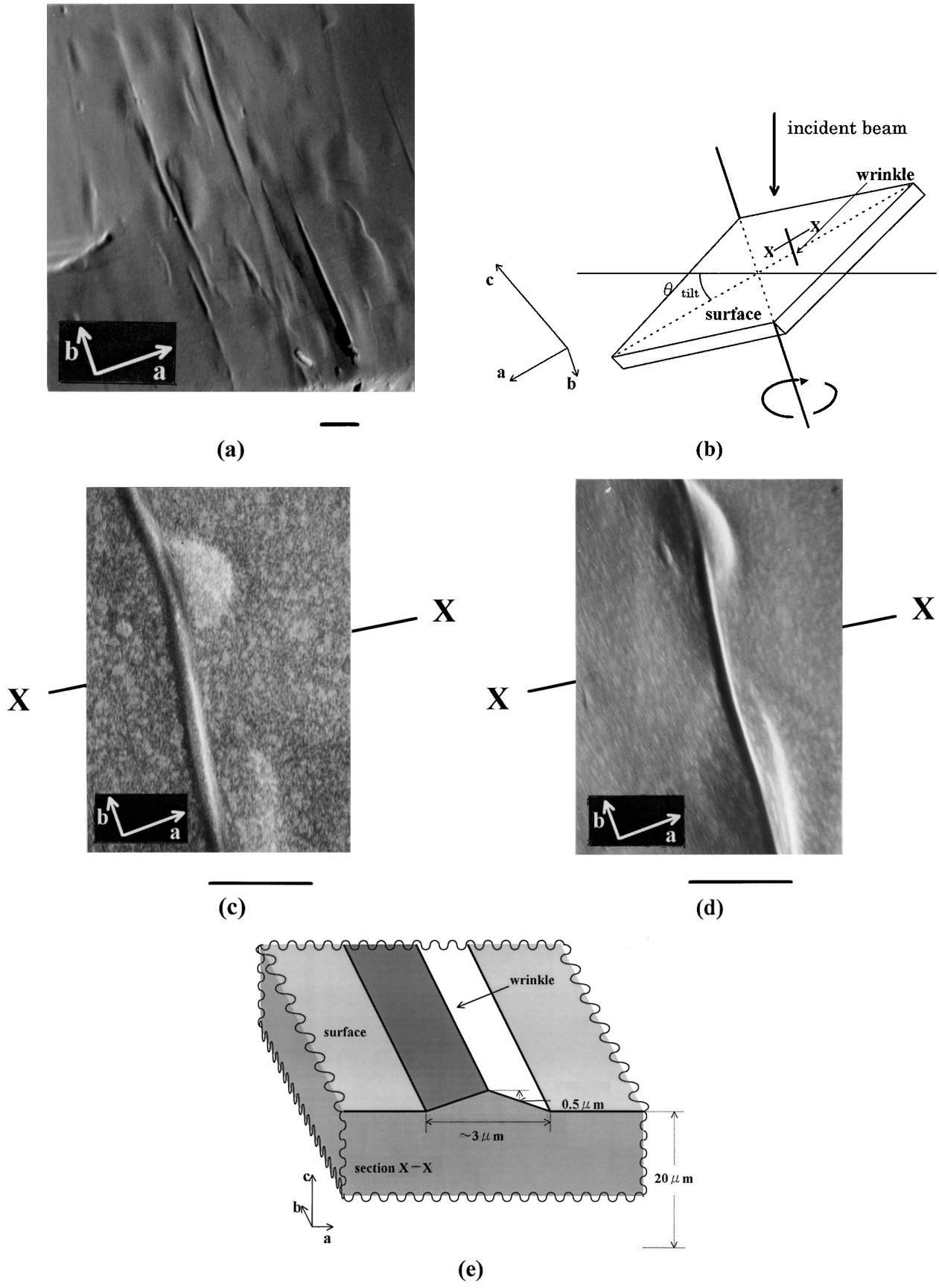

Figure 7 (a) SEM image of the typical wrinkles. Scale bar = 10 μm. (b) Geometry of the SEM observation method for the investigation of the structure detail of the wrinkle. (c), (d) SEM image of the typical wrinkle observed by the method shown in (b) with (c) $\theta_{tilt} = 20^\circ$ and (d) 60°, respectively. In both images, scale bar = 10 μm. (e) Schematic illustration of the morphology of the typical wrinkle.

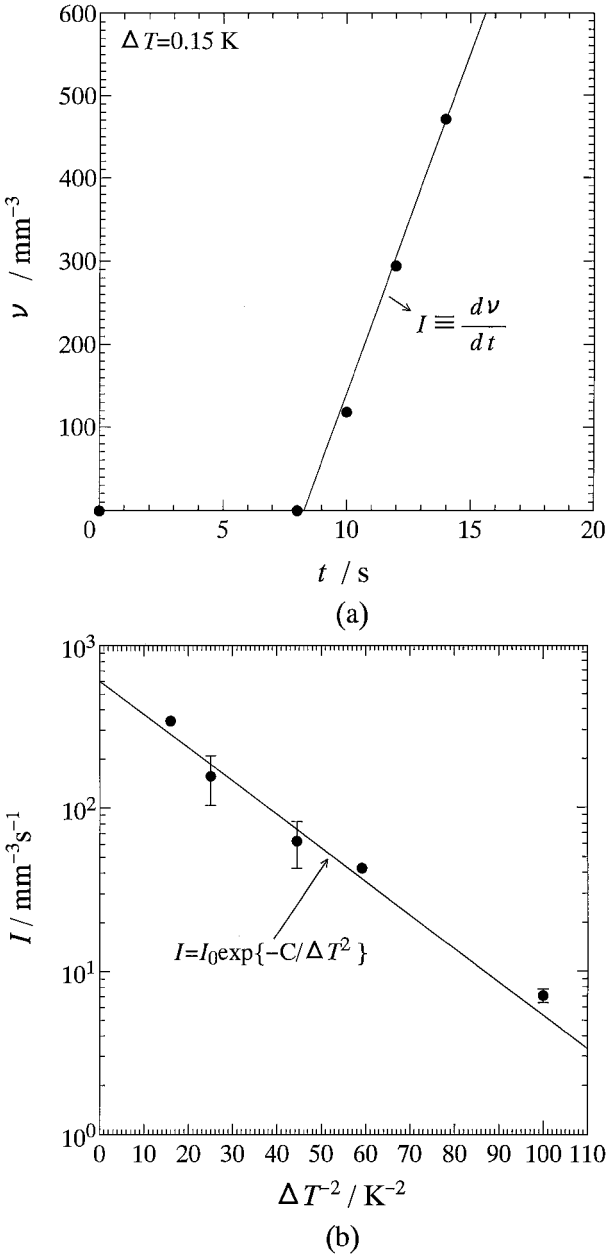

Figure 8 (a) Density of the primary nucleus of the R phase vs. time at 46.45°C ($\Delta T = 0.15$ K). (b) Primary nucleation rate I in log scale vs. ΔT^{-2}. The data lie approximately on a linear line.

to be transition temperature and is approximately equal to the equilibrium transition temperature T_{LO-R}.

We must recall the effect of the homologous impurity here. If the sample contains the homologous impurity, it allows the coexistence of the LO phase and the R phase even at a temperature below the equilibrium transition temperature of the pure sample. The range of coexisting temperature is roughly estimated to be less than 0.1°C for the homologous impurity of 0.4 wt% [19]. Therefore if the temperature (T_w) where the wrinkle first appears on heating ($T_w = 45.8$°C) is regarded as the lowest temperature of coexisting temperature (T_l), i.e. $T_w = T_l$, the highest one (T_h) should be $T_h \leq 45.9$°C. In this case, $T_{LO-R} = 46.3$°C is 0.4°C higher than T_h, so at any higher temperature than T_{LO-R}, the wrinkle should be completely in the R phase. Therefore the R phase should grow from all wrinkles. However it could be confirmed that there were some wrinkles from which the R phase did not grow during the observation even at a temperature above 46.4°C. Thus, we can logically conclude that the appearance of the wrinkle is a kind of precursor of the LO-R transition.

Unfortunately this logic can not be confirmed experimentally, because it is difficult to distinguish if the wrinkle is in the LO phase or in the R phase by means of X-ray diffraction or DSC method. Thus there remains a little possibility that the wrinkle is due to a kind of impurity effect. Furthermore, the 'air effect' must be considered, too. Sirota, *et al.* reported that air was soluble in the R phase [27], which may have a similar effect on the LO-R transition. Therefore, in order to prove this conclusion of the precursor wrinkle exactly, further investigation will be necessary and performed in future.

4.2. Origin of the wrinkle

Fig. 9a and b show a mechanism of the formation of the wrinkle on the basis of the assumption that it is the precursor of the LO-R transition. Many defects were considered to be formed during the crystallization from the solution. It is well-known that the thermal expansion coefficient β of amorphous is usually much larger than that of crystal. From analogy of this, β around the defect

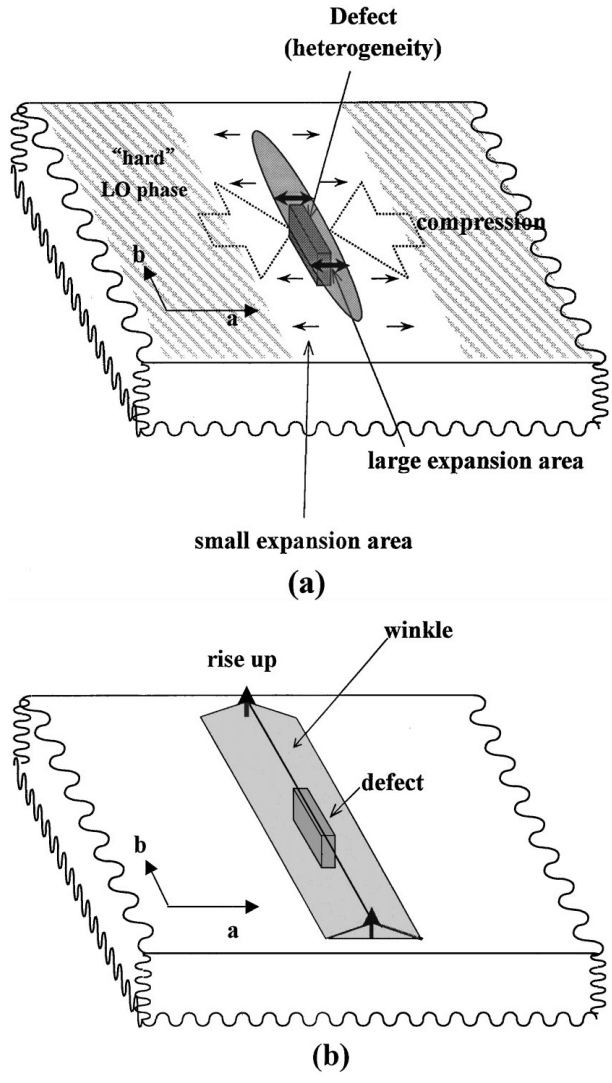

Figure 9 A model of the formation of the wrinkle prior to the R phase transition in a single crystal of *n*-alkane: (a) before the formation and (b) after the formation of the wrinkle.

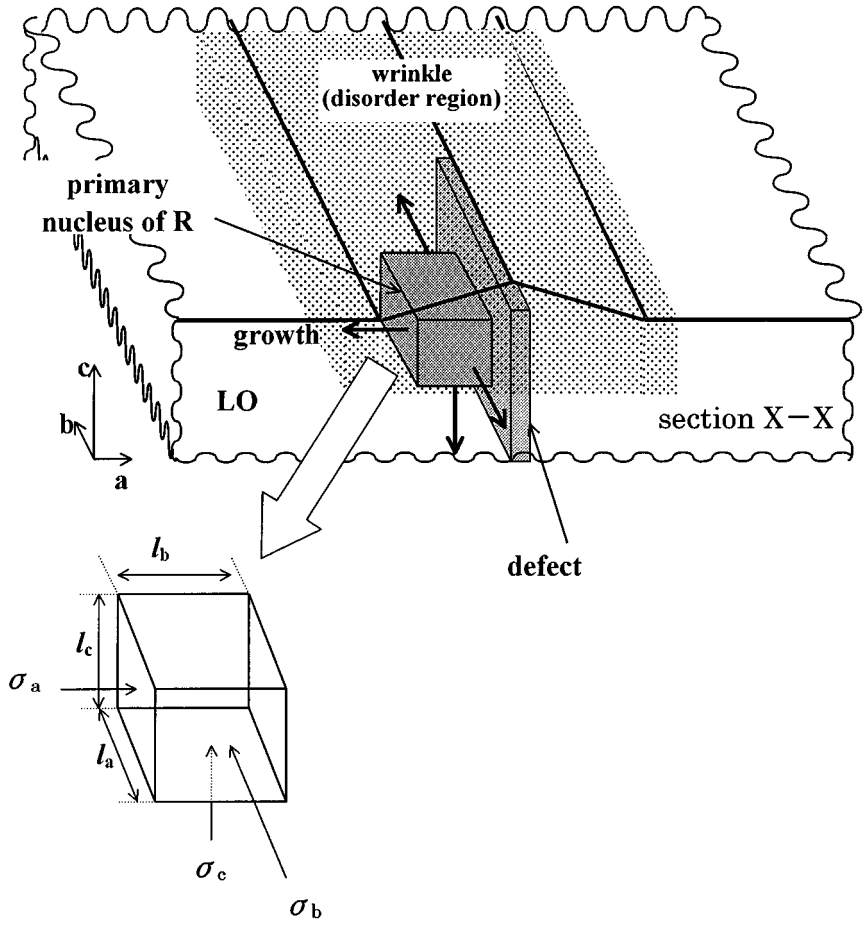

Figure 10 Schematic illustration of the primary nucleus in the wrinkle region. The section X-X corresponds to that in Fig. 7. The defect plays a role as a nucleation agent in this case.

should be larger than that in ordered region. Therefore, the defects cause significant lattice expansion within a single crystal, resulting in the local accumulation of the strain within the 'large expansion area' in Fig. 9a. The accumulated strain may be anisotropic due to large β along *a* axis than that along *b* axis shown in Fig.2b. With an increase in temperature, the strain will increase. The large expansion area is surrounded by the 'hard' LO phase, resulting in suffering compression along the *a* axis. When the accumulated strain reaches a critical barrier, the wrinkle will be formed at the defect to relax the strain partially (Fig. 9b). This is the reason why the wrinkles always appear at the same position. The significant anisotropic expansion makes the wrinkles parallel to the *b* axis. This mechanism can well explain the temperature dependence of the wrinkle density (Fig. 6) among the different samples measured here. The increase in lattice constant only depends on temperature. Therefore, the wrinkle density may only depend on temperature, too, and be saturated by the finite number of the defects. If the wrinkle was the onset of the LO-R transition, this mechanism could be also applicable, because the lattice expansion is large at the transition.

This model of the origin of the wrinkle may be supported by a microscopic model proposed by Strobl *et al.* [28]. They suggested that the longitudinal motion of the molecules along the chain such as flip-flop screw jump is activated even in the LO phase. When the temperature increases up to $T_{\mathrm{LO-R}}$, the thermal motion of the molecules along the chain axes are more excited. The crystal can relax the locally accumulated strain by shifting and pushing out the molecules along their long axes, resulting in the wrinkles.

4.3. Mechanism of the primary nucleation

On heating, the primary nucleus is probably formed in the wrinkle region as shown in §Results. Fig. 10 shows a schematic drawing of the primary nucleus in the wrinkle. The structure is disordered and a little strain may remain in the wrinkle region.

When the R phase nucleates primarily, the defect may play a role as an nucleation agent. In the wrinkle, because of the disordered structure, the nucleation barrier is lower than that in other region. Hence, the primary nucleation rate is larger. This is the reason why the primary nucleation is expected to occur selectively in the wrinkle. In this case of the heterogeneous nucleation, the defect is the heterogeneity.

4.4. Heterogeneous primary nucleation rate

The nucleation rate I is given by

$$I \propto \exp\left(-\frac{\Delta G^*}{kT}\right), \tag{3}$$

where ΔG^* is the activation free energy barrier of the critical nucleus, k is the Boltzmann constant ($k = 1.38 \times 10^{-23}\ \mathrm{J \cdot K^{-1}}$), and T is temperature [29]. In the case of the 3D nucleus shown in Fig. 10, I is given by

Equation 1. In the case of homogeneous nucleation,

$$C = \frac{32 T_{\mathrm{LO-R}} \sigma_a \sigma_b \sigma_c}{k \Delta h^2}, \tag{4}$$

where σ_a, σ_b, and σ_c are the surface free energies of the (100), (010), and (001) boundary surfaces between the LO phase and the R phase, and Δh is the enthalpy per unit volume of the R phase transition [26]. In this work, $\Delta h = 6.85 \times 10^7 \mathrm{J \cdot m^{-3}}$ is used [30].

We can calculate C for homogeneous nucleation in LO-liquid(L) transition by using the values σ_a σ_b and $\sigma_c \approx 9 \times 10^{-3}$ J $\cdot$ m^{-2} estimated from the experimental result of the crystallization of *n*-alkane [31],

$$C_{\mathrm{homo}}^{\mathrm{LO-L}} = 1.2 \times 10^6 \ \mathrm{K^2}. \tag{5}$$

This value is much larger than $C_{\mathrm{obs}} = 4.7 \times 10^{-2}$ K in Equation 2,

$$C_{\mathrm{obs}} \ll C_{\mathrm{homo}}^{\mathrm{LO-L}}. \tag{6}$$

The surface free energies used in above case corresponds to those between the LO phase and the liquid phase [31], therefore other calculation can be performed by using the values σ_b, $\sigma_c \approx 3.4 \times 10^{-4}$ J $\cdot$ m^{-2} which were estimated from the growth rate of the R phase during the R phase transition in C25 [1] and correspond to the surface free energies between the LO phase and the R phase,

$$C_{\mathrm{homo}}^{\mathrm{LO-R}} = 7.1 \ \mathrm{K^2}, \tag{7}$$

where σ_a is assumed to be approximately equal to σ_b and σ_c. In this case, the calculated C value is also much larger than the observed C value,

$$C_{\mathrm{obs}} \ll C_{\mathrm{homo}}^{\mathrm{LO-R}}. \tag{8}$$

Thus, the observed C value, C_{obs}, is too small to be concluded that the primary nucleation is homogeneous. Therefore, the primary nucleation in this case can be concluded to be heterogeneous one from the quantitative consideration of the kinetic parameter as well as from the morphological observation.

In the case of 3D heterogeneous nucleus illustrated in Fig. 10, we can derive the formulae

$$C = \frac{16 T_{\mathrm{LO-R}} \Delta\sigma_a \sigma_b \sigma_c}{k \Delta h^2}, \tag{9}$$

and

$$\Delta\sigma_a \equiv \sigma_a + \sigma_a^{\mathrm{R-defect}} - \sigma_a^{\mathrm{LO-defect}}, \tag{10}$$

where $\sigma_a^{\mathrm{R-defect}}$ and $\sigma_a^{\mathrm{LO-defect}}$ are the surface free energy of the (100) boundary surface between the R phase and the defect and that between the LO phase and the defect, respectively [26].

From Equations 2 and 10, $\Delta\sigma_a$ is estimated to be $\Delta\sigma_a = 5.9 \times 10^{-6}$ J $\cdot$ m^{-2}, where $\sigma_b\sigma_c = 1.2 \times 10^{-7}$ J^2 $\cdot$ m^{-4} which was estimated from the growth rate of the R phase in C25 is used [1]. Assuming that σ_a approximately equal to σ_b and σ_c, i.e. $\sigma_a \approx 3.4 \times 10^{-4}$ J $\cdot$ m^{-2}, we can derive the parameter $\Delta\sigma_a/\sigma_a$,

$$\frac{\Delta\sigma_a}{\sigma_a} = 1.7 \times 10^{-2}. \tag{11}$$

This value seems to be a little smaller than that obtained in the case of the heterogeneous nucleation of hexagonal crystal of polyethylene [32]. In above estimation, the effect of the nucleation in the disordered wrinkle region is not introduced. Therefore, the σ_a, σ_b and σ_c values used here may be large for the estimation in this case, because the surface free energy between the disordered LO phase and the R phase is expected to be smaller than that between the ordered LO phase and the R phase. If the effect of the nucleation in the disorder is taken into consideration, larger $\Delta\sigma_a$ value will be obtained. From Equation 3, the critical nucleation barrier ΔG^* and the sizes of the critical nucleus l_a^*, l_b^* and l_c^* are obtained,

$$\Delta G^* = 2.1 \times 10^{-22} \Delta T^{-2} \ \mathrm{J} \tag{12}$$

and

$$l_a^* = 5.5 \times 10^{-2} \Delta T^{-1} \ \mathrm{nm}, l_b^*, l_c^* = 6.6 \Delta T^{-1} \ \mathrm{nm}. \tag{13}$$

For example, at $\Delta T = 0.1$ K, $\Delta G^* = 2.1 \times 10^{-20}$ J, $l_a^* = 5.5 \times 10^{-1}$ nm and l_b^*, $l_c^* = 6.6 \times 0^1$ nm. These values are considered to be suitable for this case. ΔG^* is larger than kT for $\Delta T < 0.2$ K, suggesting that the nucleation controls the R phase transition.

4.5. Origin of the hysteresis

On heating in the R phase transition, the primary nucleus is formed in the wrinkle in which the structure is disordered and the strain is accumulated because of the hard character of the LO phase. Under such condition, the surface free energies $\Delta\sigma_a$, σ_b and σ_c are smaller than those in the ordered region, and the nucleation barrier is low, resulting in the large nucleation rate. While on cooling from the R phase, because of the 'soft' character of the R phase, the strain is not accumulated and the structure in the R phase is naturally disordered. The nucleation rate on cooling in this case is smaller than that on heating. Therefore, it is impossible that the primary nucleus is formed in a finite observation time at small ΔT_c; the supercooling of 1–2 °C is observed. When ΔT_c becomes large, the nucleus of the LO phase can be formed in the R phase, resulting in the transition. Because of the high growth rate at a large ΔT_c [1], the transition completes within short time.

In the case of cooling from the coexistent state of the LO and R phases, significant different nucleation can be expected compared with the case of cooling from the R phase. The transition does not need the primary nucleation of the LO phase but needs only 2D surface nucleation. Therefore, the transition starts at much smaller degree of supercooling. No significant hysteresis is observed.

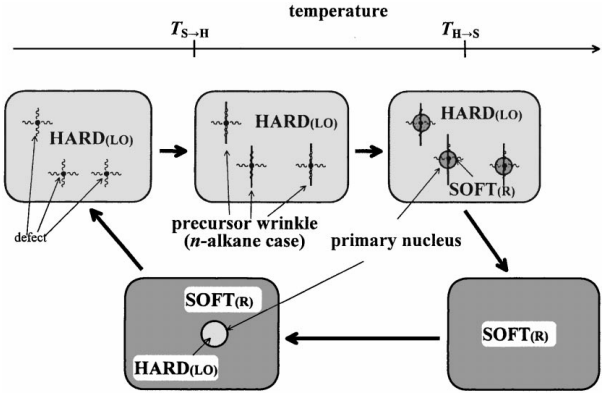

Figure 11 Schematic picture of the universal mechanism of the common hysteresis in the first-order phase transition of materials.

The universal mechanism of the hysteresis in the first-order transition can be proposed and is shown in Fig. 11. The crystal in the low-temperature 'hard' phase like the LO phase in the case of *n*-alkane probably have many defects, around which the strain is accumulated. The primary nucleus of the high-temperature 'soft' phase like the R phase in the case of *n*-alkane may be formed selectively at such defects, because the primary nucleation barrier is low around the defects. This nucleation process is heterogeneous one. In the present case of *n*-alkane, the position of the defects become visible by the formation of the wrinkle prior to the R phase transition, the nucleation at the defects can be experimentally confirmed by means of *in situ* optical microscopy.

When the hard→soft transition completes, all region of the soft phase is in uniform disordered phase. On cooling, there is nothing which accelerates the primary nucleation in the soft phase. In this case, it is natural that significant supercooling is observed. The present study could show the tangible evidence of the above universal mechanism of the hysteresis in the first-order phase transition of materials.

5. Conclusions

We have studied the rotator phase transition of *n*-alkane ($C_{25}H_{52}$) mainly by means of *in situ* optical microscopy. The major results are summarized as follows.

On heating, the wrinkles appear on the crystal surface at a temperature slightly below the R phase transition. The rotator phase develops from the wrinkles above the transition temperature, therefore, the primary nucleation occurs in the wrinkles. The wrinkle is the precursor of the transition and can accelerate the primary nucleation. However, it still remains another supposition that the wrinkle is the onset of the LO-R transition on the basis of the impurity effect. In order to conclude whether the precursor or the impurity effect exactly, Further investigation will be necessary.

The primary nucleation rate of the R phase was measured and was found to be proportional to $\exp(-C/\Delta T^2)$, which means that the primary nucleus is three-dimensional one. It is concluded from the results of the morphological observation and the consideration of the quantitative kinetic parameter that the R phase transition in *n*-alkane is controlled by the nucleation and growth, and that the R phase nucleates heterogeneously in the precursor wrinkle.

On cooling, no change was detected prior to the phase transition. The observed transition temperature was 1–2 °C lower than that on heating. The large difference in transition temperature between on heating and cooling was observed. Such hysteresis is widely observed in first-order phase transitions. The mechanism of the hysteresis was proposed. On heating, the primary nucleation barrier is lower around defect, because strain is accumulated around the defect within 'hard' low-temperature ordered phase. In the case of *n*-alkane, the accumulation of strain results in the visible wrinkle as a precursor of the transition. On cooling, the accumulation of strain is not occurred within 'soft' high-temperature disordered phase, therefore there is no site in which the primary nucleation barrier is lower and the nucleation rate is not large compared to that on heating. Thus, the difference in mechanism of primary nucleation between on heating and on cooling is the origin of the hysteresis. The present results could show the tangible evidence of this mechanism.

Acknowledgements

The authors are very grateful to Professor Takashi Yamamoto and Professor Tetsuhiko Hara at the Faculty of Science, Yamaguchi University, for various discussions of the results. The authors are also grateful to Dr. Yoshihiro Ogawa at the Faculty of Science, Kumamoto University, for analysis of the sample purity. Furthermore, the authors express their thanks to Mr. Koichi Onoue and Mr. Yuji Saito at Central Glass Co. Ltd. for their assistance of SEM observation. This work was supported by a Grant-in-Aid for Scientific Research from the Ministry of Education, Science, Sports, and Culture, Japan, and an international research grant (NEDO).

References

1. K. NOZAKI and M. HIKOSAKA, *Jpn. J. Appl. Phys.* **37** (1998) 3450.
2. B. WUNDERLICH, "Macromolecular Physics," Vol. 3 (Academic Press, New York, 1973), ch. 8.
3. T. YAMAMOTO, K. NOZAKI and T. HARA, *J. Chem. Phys.* **92** (1990) 631.
4. K. TAKAMIZAWA, Y. URABE, J. FUJIMOTO, H. OGATA and Y. OGAWA, *Thermochimca Acta* **267** (1995) 297.
5. B. M. CRAVEN, Y. LANGE, G. G. SHIPLEY and J. STEINER, in "Handbook of Lipid Research," Vol. 4 edited by D. M. Small (Plenum, New York, 1986).
6. M. G. BROADHURST, *J. Res. Natl. Bur. Stand. Sect. A* **66** (1962) 241.
7. A. MÜLLER, *Proc. R. Soc. London Ser. A* **138** (1932) 514.
8. J. DOUCET, I. DENICOLO and A. GRAIEVICH, *J. Chem. Phys.* **75** (1981) 1523.
9. J. DOUCET, I. DENICOLO, A. GRAIEVICH and A. COLLET, *ibid.* **75** (1981) 5125.
10. I. DENICOLO, J. DOUCET and A. F. GRAIEVICH, *ibid.* **78** (1983) 1465.
11. J. DOUCET, I. DENICOLO, A. F. GRAIEVICH and C. GERMAIN, *ibid.* **80** (1984) 1647.
12. G. UNGAR, *J. Phys. Chem.* **87** (1983) 689.
13. G. UNGAR and MAŠIĆ, *ibid.* **89** (1985) 1036.
14. E. B. SIROTA, H. E. KING Jr., D. M. SINGER and H. H. SHAO, *J. Chem. Phys.* **98** (1993) 5809.
15. E. B. SIROTA and D. M. SINGER, *ibid.* **101** (1996) 10873.

16. T. YAMAMOTO and K. NOZAKI, *Polymer* **35** (1994) 3340.
17. *Idem., ibid.* **36** (1995) 2505.
18. T. YAMAMOTO, T. AOKI, S. MIYAJI and K. NOZAKI, *ibid.* **38** (1997) 2643.
19. For example, M. DIRAND, Z. ACHOUR, B. JOUTI and A. SABOUR, *Mol. Cryst. Liq. Cryst.* **275** (1996) 293.
20. H. LUTH, S. C. NYBERG, P. M. ROBINSON and H. G. SCOTT, *ibid.* **22** (1972) 337.
21. K. TAKAMIZAWA, T. SONODA and Y. URABE, *Engineering Science Reports of Kyusyu University* **10** (1989) 363 (in Japanese).
22. K. NOZAKI, N. HIGASHITANI, T. YAMAMOTO and T. HARA, *J. Chem. Phys.* **103** (1995) 5762.
23. Y. URABE and K. TAKAMIZAWA, *Technology Reports of Kyusyu University* **67** (1994) 85 (in Japanese).
24. W. PIESCZEK, G. STROBL and K. MALZAHN, *Acta Crystallogr. Sect. B* **30** (1974) 1728.
25. K. NOZAKI, T. YAMAMOTO, T. HARA and M. HIKOSAKA, *Jpn. J. Appl. Phys.* **36** (1997) L146.
26. F. D. PRICE, "Nucleation" (Marcel Dekker, New York, 1969), ch. 8.
27. E. B. SIROTA, D. M. SINGER and H. E. KING Jr., *J. Chem. Phys.* **100** (1994) 1542.
28. G. STROBL, B. EWEN, E. W. FISCHER and W. PIESCZEK, *ibid.* **61** (1974) 5257.
29. D. TURNBULL and J. C. FISHER, *ibid.* **17** (1949) 71.
30. A. WURFLINGER and G. M. SCHNEIDER, *Ber. Bunsenges. Phys. Chem.* **77** (1973) 121.
31. D. TURNBULL and R. L. CORMIA, *J. Chem. Phys.* **34** (1961) 820.
32. M. NISHI, PhD thesis, Hiroshima University, Japan 1998.

Received 8 December 1998
and accepted 25 August 1999